Available online at www.sciencedirect.com
ScienceDirect
Journal of Power Sources 172 (2007) 666–675
JOURNAL OF POWER SOURCES
www.elsevier.com/locate/jpowsour

The durability of polyol-synthesized PtRu/C for direct methanol fuel cells

Junsong Guo [a], Gongquan Sun [a,*], Zhimou Wu [a], Shiguo Sun [a], Shiyou Yan [a], Lei Cao [a], Yushan Yan [b], Dangsheng Su [c], Qin Xin [a]

[a] *Direct Methanol Fuel Cell Laboratory, Dalian Institute of Chemical Physics, Chinese Academy of Sciences, Dalian 116023, China*
[b] *Department of Chemical and Environment Engineering, University of California, Riverside, CA 92521, USA*
[c] *Department of Inorganic Chemistry, Fritz-Haber Institute of the Max Planck Society, Berlin D-14195, German*

Received 27 March 2007; received in revised form 7 May 2007; accepted 8 May 2007
Available online 13 May 2007

Abstract

The durability of polyol-synthesized PtRu/C as anode electrocatalyst for direct methanol fuel cells (DMFCs) has been studied by conducting a 2020-h life-test of a single cell discharging at a constant current density of 100 mA cm^{-2}. Critical fuel cell performance parameters including anode activity, cathode activity and internal resistance are, for the first time, systematically examined at the life-test time of 556, 1093, 1630 and 2020 h. High-resolution transmission electron microscopy and X-ray diffraction (XRD) have also been performed and show that PtRu nanoparticles have agglomerated with the mean particle size increasing from 1.82 to 2.78 nm after the 2020-h life-test. Anode polarization and electrochemical impedance spectroscopy (EIS) show that there exists a stable discharging period where the anode polarization potential is less than 0.363 V versus dynamic hydrogen electrode (DHE). When the anode polarization potential exceeds 0.363 V versus DHE, the performance of the anode degrades dramatically due to the leaching of the unalloyed Ru as indicated by energy dispersive X-ray spectroscopy (EDS) and XRD. This finding provides clues in developing strategies to operate fuel cells achieving maximum lifetime without noticeable performance lose.

Keywords: Direct methanol fuel cell; PtRu; Durability; Unalloyed Ru

1. Introduction

Direct methanol fuel cells (DMFCs) have received much attention due to their great promise as a high energy density, long-life and instantaneously rechargeable power source for portable electronic devices [1,2]. Although the successful implementation of DMFCs critically depends on the long-term durability of its electrocatalysts, systematic studies on durability of electrocatalysts are scarce because of the time and efforts required. Consequently, the mechanisms of the catalyst activity loss are still unclear.

At present, platinum and ruthenium supported on carbon (PtRu/C) catalysts are the most effective anode catalysts for DMFCs. The limited number of life-test studies of this catalyst system include a 2000-h life-test by Thomas et al. [3], a 1002-h life-test by Cheng et al. [4], a 500-h life-test by Chen et al. [5] and a 75-h life-test by Liu et al. [6]. All of these studies have been limited to the recording of performance of the single cell at a constant current or constant voltage discharge, followed by a post-mortem examination of metal particle size and chemical composition so that Ru leaching can be identified. Gradual leaching of Ru has been considered as the main reason for the activity loss of PtRu/C in addition to the aggregation of metal particles. Taniguchi et al. [7] have found severe Ru loss especially in the fuel outlet region. The studies by Cheng et al. [4] have revealed that the amount of Ru in PtRu black decreases from 46.8% to 34.4% after a 1002-h life-test. Ru-leaching is also observed after a 500-h life-test in our previous work [5]. Subsequently, Chen et al. [8] have found that the stability of anode catalysts closely depends on the anode potential by potential scan method, and that Ru in PtRu/C catalyst begins to dissolve when the anode potential value exceeds 0.6 V versus dynamic hydrogen electrode (DHE). Moreover, the degradation rates of performance are observed to be different from various life-tests. Chen et al. [5] have found that the loss of peak power density of the DMFC with a homemade PtRu/CNTs (CNTs for carbon nanotubes) as anode catalyst is about 16.3% after a 500-h life-test under a discharging current density of 70 mA cm^{-2}, whereas

* Corresponding author. Tel.: +86 411 84379063; fax: +86 411 84379063.
E-mail address: gqsun@dicp.ac.cn (G. Sun).

0378-7753/$ – see front matter © 2007 Elsevier B.V. All rights reserved.
doi:10.1016/j.jpowsour.2007.05.012

a 30% drop of the peak power density has been observed for a DMFC with commercial PtRu/C anode catalyst after only a 75-h life-test under a discharging current density of 100 mA cm^{-2} by Liu et al. [6]. In addition, even in the same single cell, different degradation rates have been observed at various discharging times [4]. All of these results indicate that anode catalysts working under different potentials have different degradation rates. Thus, finding out the suitable anode working potential to avoid the leaching of Ru could be critical to improve the durability of DMFCs.

Leached Ru could migrate across the Nafion membrane to cathode and inhibits the oxygen reduction reaction (ORR) of the cathode, as found by Piela et al. [9]. Therefore, the degradation of PtRu/C not only reduces the activity of anode, but also likely reduces the activity of the cathode. Furthermore, it is known that the Ru in PtRu/C exists in both alloyed form and the amorphous form [10], and the later usually consists of ruthenium oxides or hydrous ruthenium oxides (RuO_xH_y), which could play a role in conducting protons and reducing the methanol oxidation potential on Pt [11,12]. Thus, the degradation of PtRu/C can be likely reflected on the value of internal resistance of the single cell.

Based on the above discussion, changes of activity of anode, activity of cathode and internal resistance are expected during the life-test. However, these three factors have not been systematically studied by conducting a comprehensive long life-test of a DMFC under real working conditions, even though they have fundamental influences on the overall performance of a DMFC, and have the potential to reveal insights in developing strategies to operate the fuel cell with a given anode catalyst to maximize the lifetime of the fuel cell.

In this paper, 45%PtRu/XC-72 (45 mass% metal supported on Vulcan XC-72 carbon black with nominal Pt:Ru atomic ratio of 1:1) prepared by modified glycol method and 40%Pt/XC-72 (JM) (40 mass% metal supported on Vulcan XC-72 carbon black, purchased from Johnson Matthey Corp.) have been used as anode and cathode catalysts for a DMFC, respectively. A 2020-h life-test has been conducted in a single cell to study the degradation of the DMFC discharging at a current density of 100 mA cm^{-2}. At the test time of 0, 556, 1093, 1630 and 2020 h, the internal resistance, anode/cathode polarization and electrochemical surface area of anode/cathode have been characterized. After life-test, the morphology, alloying degree, elemental composition and distribution of catalysts before and after the life-test have been investigated. The factors causing the performance decay of the DMFC and the strategies to operate a DMFC to maximize the lifetime are discussed.

2. Experiment

2.1. Anode catalyst preparation

$H_2PtCl_6{\cdot}6H_2O$ and $RuCl_3$ were used as precursors for the PtRu catalyst. Vulcan XC-72 carbon black (Cabot Corp. $S_{BET} = 236.8\ m^2\ g^{-1}$) oxidized by concentrated H_2O_2 was used as the catalyst support. The 45%PtRu/XC-72 catalyst was prepared via the following procedure. Calculated $H_2PtCl_6{\cdot}6H_2O$ and $RuCl_3$ were added to the ethylene glycol to form a brown solution with 2 mg metal mL^{-1} solvent. Then the pH value of the solution was increased to above 13 with a solution of sodium hydroxide in ethylene glycol and the solution was heated to 170 °C at a rate of 10 °C min^{-1} and kept at this temperature for 3 h to obtain a brown–black sol. At this time, a calculated amount of XC-72 carbon black was added to the above sol and stirred for half an hour. Then the above solution was cooled to room temperature, and an appropriate amount of diluted hydrochloric acid was added to adjust the pH value to below 3. The solution was stirred for 12 h to settle the PtRu nanoparticles. The final catalyst was then filtered, washed and dried.

2.2. Membrane electrode assembly (MEA) and single cell fabrication

The MEA was fabricated according to the method in the literature [13]. The 45%PtRu/XC-72 catalyst was used as the anode catalyst with electrode PtRu loading of 2.0 mg cm^{-2}. And the 40%Pt/XC-72 (JM) catalyst served as the cathode catalyst with the electrode Pt loading of 1.4 mg cm^{-2}. The MEA was sandwiched between two stainless steel flow field plates to form a single cell with an active electrode area of 4 cm^2.

2.3. Life-test of a DMFC

The life-test of a DMFC was carried out using an automatic fuel cell test system (Arbin Instrument Corporation). The anode was fed with 1 mol L^{-1} methanol solution with a flow rate of 1 mL min^{-1} by a peristaltic pump without back pressure. The cathode was fed with non-humidified oxygen with a flow rate of 60 standard cubic centimeter per minute (sccm) at a pressure of 0.2 MPa. The cell was discharged in a galvanostatic mode with the current density of 100 mA cm^{-2}. The life-test time and the corresponding cell voltage were recorded. After about every 12 h or more discharge, the DMFC was duty off for resting half an hour with deflating oxygen at 0 MPa.

2.4. Electrochemical characterization

Electrochemical impedance spectroscopy (EIS), anode polarization, anode methanol stripping and cathode cyclic voltammetry were carried out at 0, 556, 1093, 1630 and 2020 h of life-test. Anode polarization and methanol striping voltammetry were performed using a potentiostat/galvanostat (EG&G Model 273A). EIS was performed using a lock-in amplifier (EG&G Model 5210) coupled to the potentiostat/galvanostat (EG&G Model 273A). The above three electrochemical experiments were carried out at 75 °C, with the anode side fed with 1 mol L^{-1} methanol at 1 mL min^{-1}, and the cathode fed with humidified hydrogen at 0.1MPa at a flow rate of 60 sccm serving as both reference and counter electrode, designated as a DHE.

2.4.1. EIS

While the anode potential was maintained at 0.350 V versus DHE, impedance spectra were recorded at 10 points per

decade by superimposing 10 mV ac signal on the cell under potentiostatic mode over the frequency range from 5 k to 0.1 Hz.

2.4.2. Anode polarization voltammetry

The anode potential was scanned at 1 mV s^{-1} starting at 0 V versus DHE and ending until current reached 1 A.

2.4.3. Methanol striping voltammetry

The anode potential was held at 0.1 V versus DHE for 40 min. During the first 20 min, methanol was adsorbed onto the anode which was fed with 1 mol L^{-1} methanol at a flow rate of 1 mL min^{-1}. During the second 20 min, the anode was washed with de-ionized water at a flow rate of 4 mL min^{-1} to remove un-adsorbed methanol. Then the anode potential was cycled between 0.1 and 0.7 V versus DHE at 20 mV s^{-1} for five cycles, and the first and fifth cycle were recorded.

2.4.4. Cathode cyclic voltammetry

The experiments were carried at 75 °C, with the cathode fed with de-ionized water at 1 mL min^{-1}, and the anode fed with humidified hydrogen at 0.1 MPa at a flow rate of 60 sccm serving as both reference and counter electrode, also designated as a DHE. Then the cathode potential was cycled between 0 and 1.2 V versus DHE at 20 mV s^{-1} for five cycles, and the fifth cycle was recorded.

2.4.5. Single cell performance test

The experiments were performed at 75 °C using an automated fuel cell test system from Arbin Instruments. The anode was fed with 1 mol L^{-1} methanol at a flow rate of 1 mL min^{-1} without backing pressure. The cathode was fed with non-humidified oxygen with a flow rate of 200 sccm at a pressure of 0.2 MPa.

2.5. Physicochemical characterization

Physicochemical characterizations of the electrocatalysts scraped from catalyst layer after the 2020-h life-test were carried out as follows. X-ray diffraction (XRD) patterns were recorded with a Rigaku Rotalflex (RU-200B) diffractometer using Cu Kα radiation with a Ni filter to study the structure of catalysts. The tube current was 100 mA with a tube voltage of 40 kV. The 2θ angular regions between 20° and 85° were explored at a scan rate of 5° min^{-1}. The morphology, microstructure and element distribution of catalysts were investigated by using Tecnai F30 field emission high-resolution transmission electron microscope (HRTEM) (FEI Company) or Hitachi H-600 integrated with energy dispersive X-ray spectroscopy (EDS).

3. Results and discussion

The result of a 2020-h life-test of the single DMFC at 100 mA cm^{-2} is shown in Fig. 1. In the process of the life-test, the continuous discharge has been periodically interrupted for the single cell resting half an hour when the discharging time is over 12 h. It can be seen that the cell voltage gradually drops during each continuous period of discharging due to inhibition of oxygen reduction reaction on the cathode caused by the Pt surface oxide (and/or hydroxide) leading to a decrease in the number of free (i.e., reduced) Pt sites [14]. This performance loss can be fully recovered during the initial 1093 h by deflating oxygen to complete reduction of the surface Pt oxide as shown in Fig. 1. But after 1093 h, the cell voltage gradually decreases and hardly restores the original level, with the voltage dropping rate increasing with test time. This irreversible performance loss must derive from the degradation of anode.

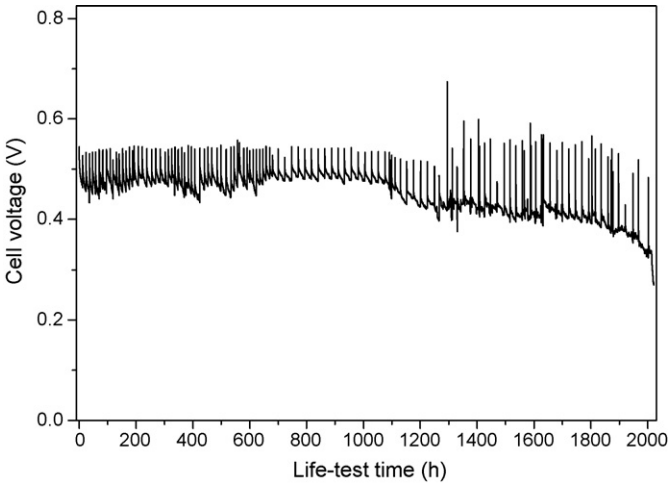

Fig. 1. Durability test of the single DMFC. Discharging current density: 100 mA cm^{-2}; cell temperature: 75 °C; anode: 1 mol L^{-1} CH_3OH at a flow rate of 1.0 mL min^{-1}; cathode: non-humidified oxygen at pressure of 0.2 MPa at a flow rate of 60 sccm.

The anode polarization curves of the DMFC after different discharging times are shown in Fig. 2. With life-test time increasing, the anode potential at the same current density moves to more positive potential, which implies that the activity of anode catalyst has degraded. When life-test time reaches 1630 and 2020 h, a limiting current appears in the end curve, which is caused by the decrease of electrochemical surface area of the electrodes due to agglomeration of catalysts. Moreover, it is

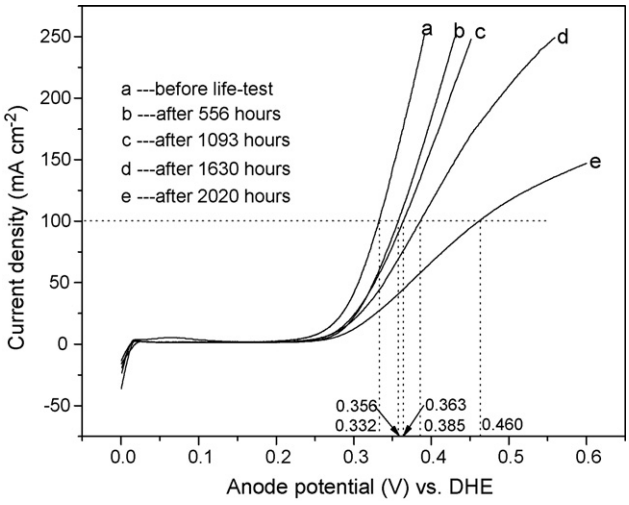

Fig. 2. Anode polarization curves at different life-test times. Cell temperature: 75 °C; scan rate: 1 mV s^{-1}; anode: 1 mol L^{-1} CH_3OH at a flow rate of 1.0 mL min^{-1}; cathode: humidified hydrogen under pressure of 0.1 MPa at a flow rate of 60 sccm.

Table 1
Fitting parameters using the equivalent circuit in Fig. 3b at different life-test times

Test time (h)	R_1 ($\Omega\,cm^2$)	C ($F\,cm^{-2}$)	R_2 ($\Omega\,cm^2$)	R_3 ($\Omega\,cm^2$)	L ($H\,cm^2$)	$R_1 \times C$ ($\Omega\,F$)
0	0.1790	0.3462	1.7570	0.3799	0.2156	0.0620
556	0.2671	0.2361	2.4640	0.6129	0.5697	0.0631
1093	0.3045	0.2179	2.5400	0.7204	0.6172	0.0664
1630	0.4392	0.1751	3.4310	1.4010	2.0470	0.0769
2020	0.6018	0.1323	4.3490	2.3980	4.2200	0.0796

observed that the degradation rate is different during different testing time. At the test time of 0, 556, 1093, 1630 and 2020 h, the anode potential is 332, 356, 363, 385 and 460 mV versus DHE at current density of 100 mA cm^{-2}, and the degrading rates between these test intervals are 0.045, 0.011, 0.042 and 0.19 mV h^{-1}, respectively. The above results indicate that there exists a stable discharging period under the anode potential less than 0.363 V versus DHE. When the anode potential is over 0.363 V versus DHE, the DMFC performance becomes more and more unstable.

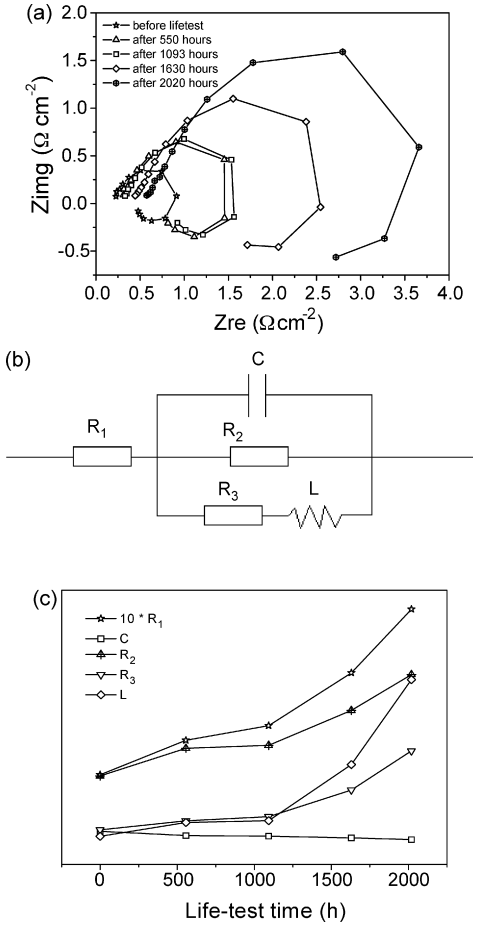

Fig. 3. (a) Electrochemical impedance spectra at different life-test times, cell temperature: 75 °C; anode: 1 mol L^{-1} CH_3OH at a flow rate of 1.0 mL min^{-1}; cathode: humidified hydrogen under the pressure of 0.1 MPa at a flow rate of 60 sccm; anode potential: 0.350 V vs. DHE, (b) equivalent circuit for modeling the faradaic impedance of methanol electrooxidation and (c) fitting parameters plots at different life-test times.

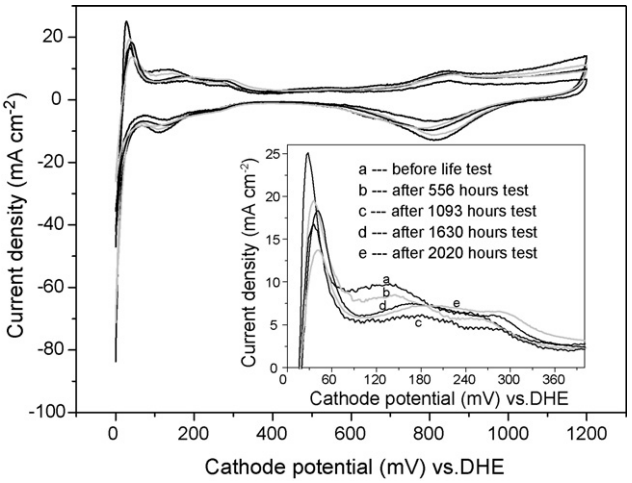

Fig. 4. Cathode cyclic voltammetry curves at different life-test times. Cell temperature: 75 °C; scan rate: 20 mV s^{-1}; anode: humidified hydrogen at pressure of 0.1 MPa with a flow rate of 60 sccm; cathode: de-ionized water at a flow rate of 1 mL min^{-1}.

Fig. 3a shows the impedance spectra at the potential of 0.350 V versus DHE at different life-test times. With the assumption that the mass transport limitations do not occur, the measured impedance spectra can be modeled by the equivalent circuit as shown in Fig. 3b [15]. The fitting parameters using the equivalent circuit in Fig. 3b are listed in Table 1, and are further

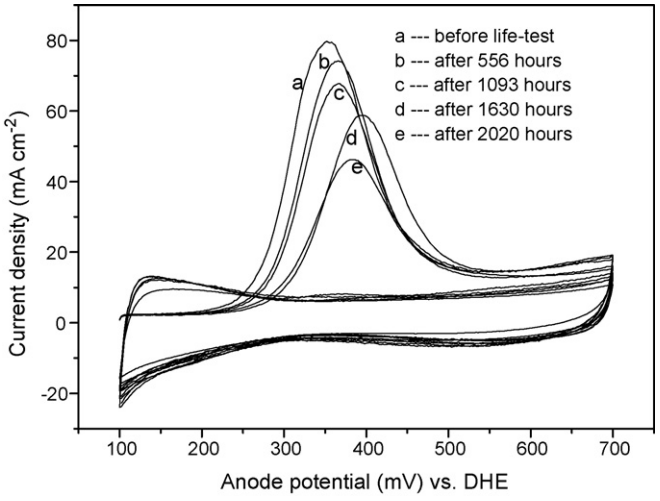

Fig. 5. Methanol stripping curves of anode at different life-test times. Cell temperature: 75 °C; scan rate: 20 mV s^{-1}; anode: 1 mol L^{-1} CH_3OH at a flow rate of 1.0 mL min^{-1}; cathode: humidified hydrogen at pressure of 0.1 MPa with a flow rate of 60 sccm.

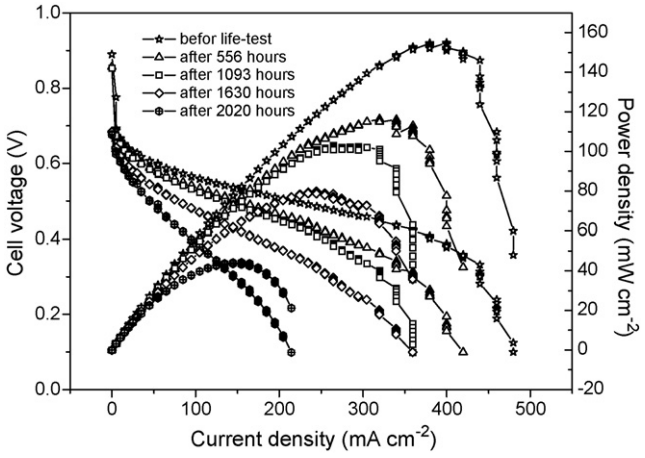

Fig. 6. Single cell performances at different life-test times. Cell temperature: 75 °C; anode: 1 mol L^{-1} CH_3OH at a flow rate of 1.0 mL min^{-1}; cathode: non-humidified oxygen at pressure of 0.2 MPa with a flow rate of 200 sccm.

plotted versus test time as shown in Fig. 3c. Here, R_1 is the internal resistance of fuel cell, R_2 the charge-transfer resistance at the interface of catalysts layer and C is the pseudo-capacitance which is related to the morphological properties of the electrochemical double layer of the electrode and to the absorption phenomena. In the simulation, the capacitance is replaced by a constant-phase element due to the porous electrode. The L, inductance at low frequencies, which means the current signal follows a voltage perturbation with a phase delay, is due to the slowness of relaxation of $(CO)_{ads}$ (adsorbed CO species) coverage, and not to parasitic electrochemical reaction for proton reduction. R_3 serves to modify the phase-delay due to the $(CO)_{ads}$ coverage relaxation process. From the results plotted in Fig. 3c, the pseudo-capacitance is decreasing because of the shrinking of the electrochemical surface area, and the internal resistance and charge-transfer resistance are increasing during the life-test, which indicates the decay of the anode. But, there exists a distinct period between 556 and 1093 h where the changes of fitting parameters are small, and the anode almost does not decay.

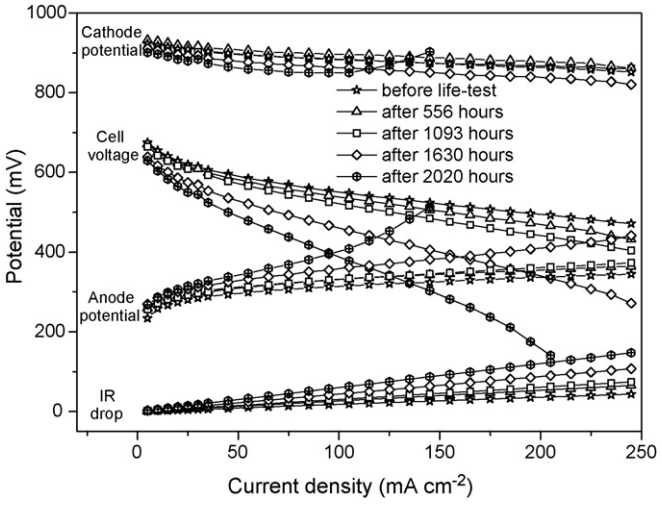

Fig. 7. Anode polarization (IR free), cathode polarization, IR drop and single cell performance at different life-test times.

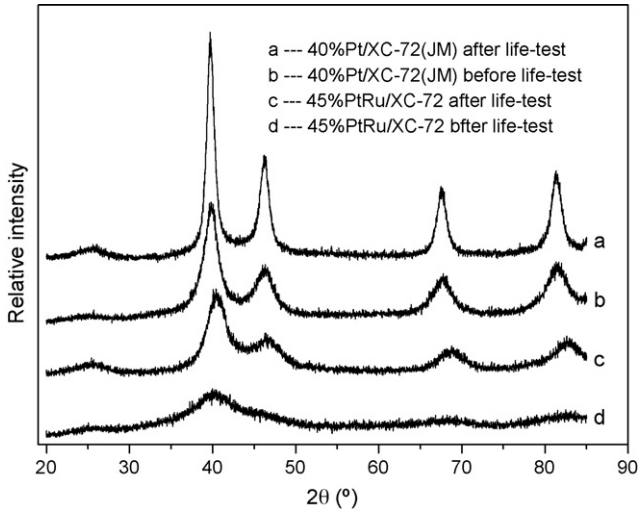

Fig. 8. XRD patterns of anode and cathode catalysts before and after 2020-h life-test.

When discharging time is over 1100 h, the fitting parameters of R_2, R_3 and L relating to methanol oxidation increase dramatically, which implies the active composition of the anode has changed. According to the results of EDS and XRD described in the latter section, the reason is likely that unalloyed Ru gradually leaches from PtRu/C when anode potential is over 0.363 V versus DHE. Unalloyed Ru supported on carbon support can reduce the methanol oxidation potential on Pt, which has been confirmed by Dubau et al. [12] and Cao et al. [16].

Moreover, by comparing the values of $R_1 \times C$ at different test times, the increase of internal resistance during the discharging time less than 1093 h is mainly due to the decrease of the contact areas between metal particles with carbon support and Nafion ionomer. If the increase of the internal resistance is merely due to the decrease of contact areas, the value of $R_1 \times C$ will stay constant. However, when the discharging time is over 1093 h (i.e., 1630 and 2020 h), the values of $R_1 \times C$ are obviously greater than those at 0, 556 and 1093 h, indicating that the loss of proton-conducting unalloyed Ru which is constituted by amorphous RuO_x [17], such as hydrous ruthenium oxides (RuO_xH_y), is another cause of the increase of the internal resistance. So, this finding can explain the phenomenon that the degradation of a DMFC is usually accompanied by an increase of internal resistance [5,6,8], which is confirmed by the same increasing trends of R_1 and R_2 as shown in Fig. 3c. After 2020-h life-test,

Table 2
Data calculated from XRD patterns by Scherrer formula

Samples	Pt (2 2 0) position ($2\theta^\circ$)	Lattice parameter (nm)	Particle size (nm)
40%Pt/XC-72 (JM)-before test	67.64	0.3914	3.31
40%Pt/XC-72 (JM)-after test	67.56	0.3918	6.28
45%PtRu/XC-72-before test	68.40	0.3876	1.82
45%PtRu/XC-72-after test	68.77	0.3858	2.78

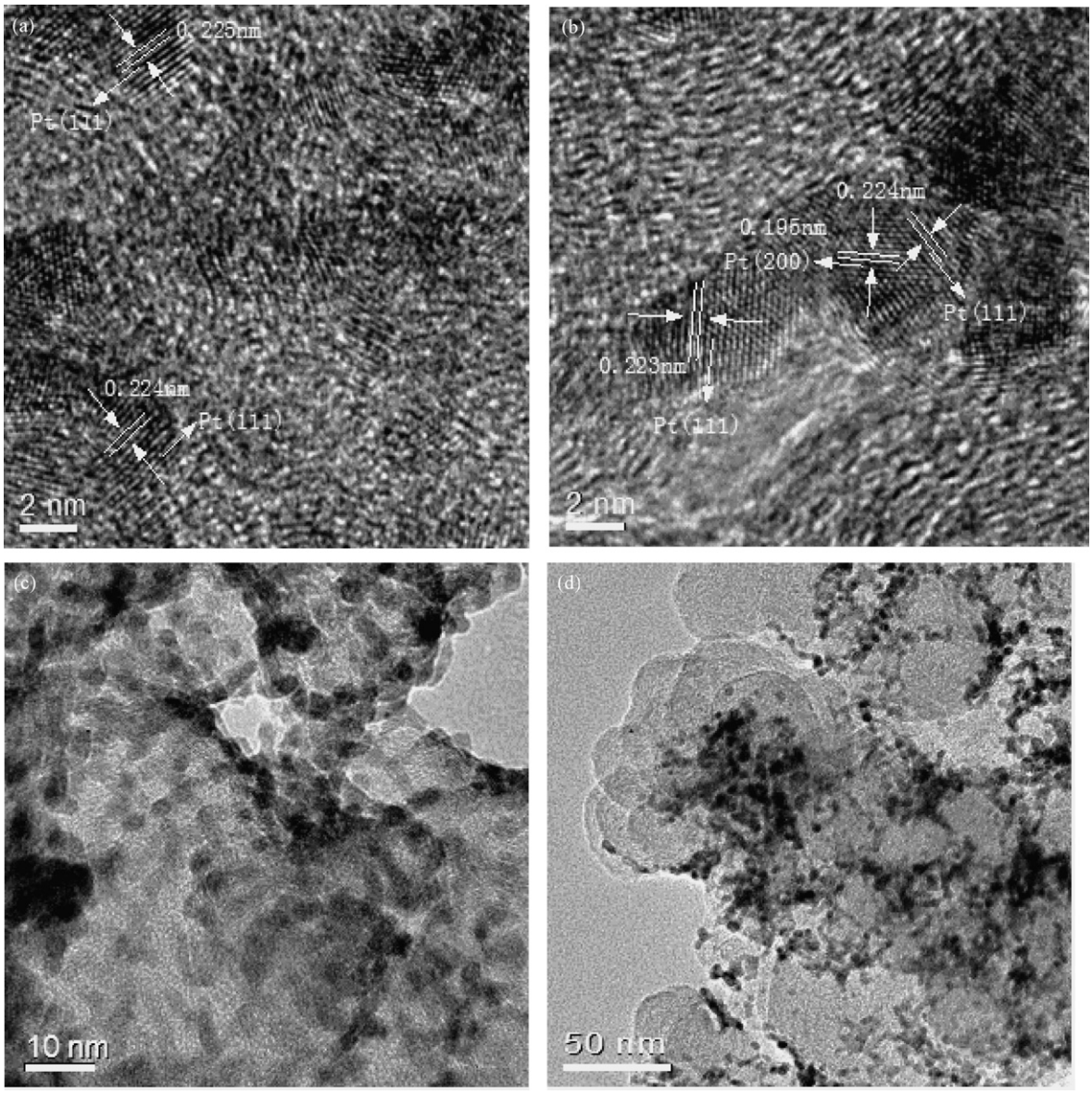

Fig. 9. HRTEM (a and b) and TEM (c and d) images of 45%PtRu/XC-72 before (a and c) and after (b and d) 2020-h life-test.

although the delamination of MEA is also observed when the single cell has been taken apart, the effect of MEA delamination on internal resistance of single cell is still unclear, especially under the pressure of two flow field plates. On the assumption that the delamination of MEA is the main reason causing the increase of internal resistance, the increasing trend of R_1 will be inconsistent with that of R_2 due to that the delamination of MEA does not affect the charge-transfer resistance at the interface of catalysts layer. However, from the results shown in Fig. 3c, R_1 and R_2 have acquired almost same increasing trend, which contradicts the deduction of this assumption, and this means that the delamination of MEA is not the main reason causing the increase of internal resistance.

The electrochemical surface areas of cathode and anode are investigated by cyclic voltammetry methods as shown in Figs. 4 and 5. The electrochemical surface area of the cathode decreases about 30% according to the hydrogen desorption peak areas calculated from Fig. 4. As for the anode catalysts, the electrochemical surface area is difficult to determine by the hydrogen desorption peak areas because of the influence of Ru. While keeping the anode under the potential of 0.1 V versus DHE, methanol molecules are adsorbed on the surface of Pt until adsorption is saturated. Later the un-adsorbed methanol molecules are purged by de-ionized water, and the adsorbed methanol molecules are almost all oxidized at the first circle. The methanol oxidization peak position and the peak area can be used to evaluate the activity and electrochemical surface area of the catalyst. From the methanol stripping curves at different test times shown in Fig. 5, the peak position shifts to higher potential and the peak area decreases with increasing test time. After 2020-h life-test, the ESA of the anode drops about 42%.

The single cell performances at 75 °C after different life-test times are shown in Fig. 6. Without considering the mass transportation polarization, anode polarization (IR free), cathode

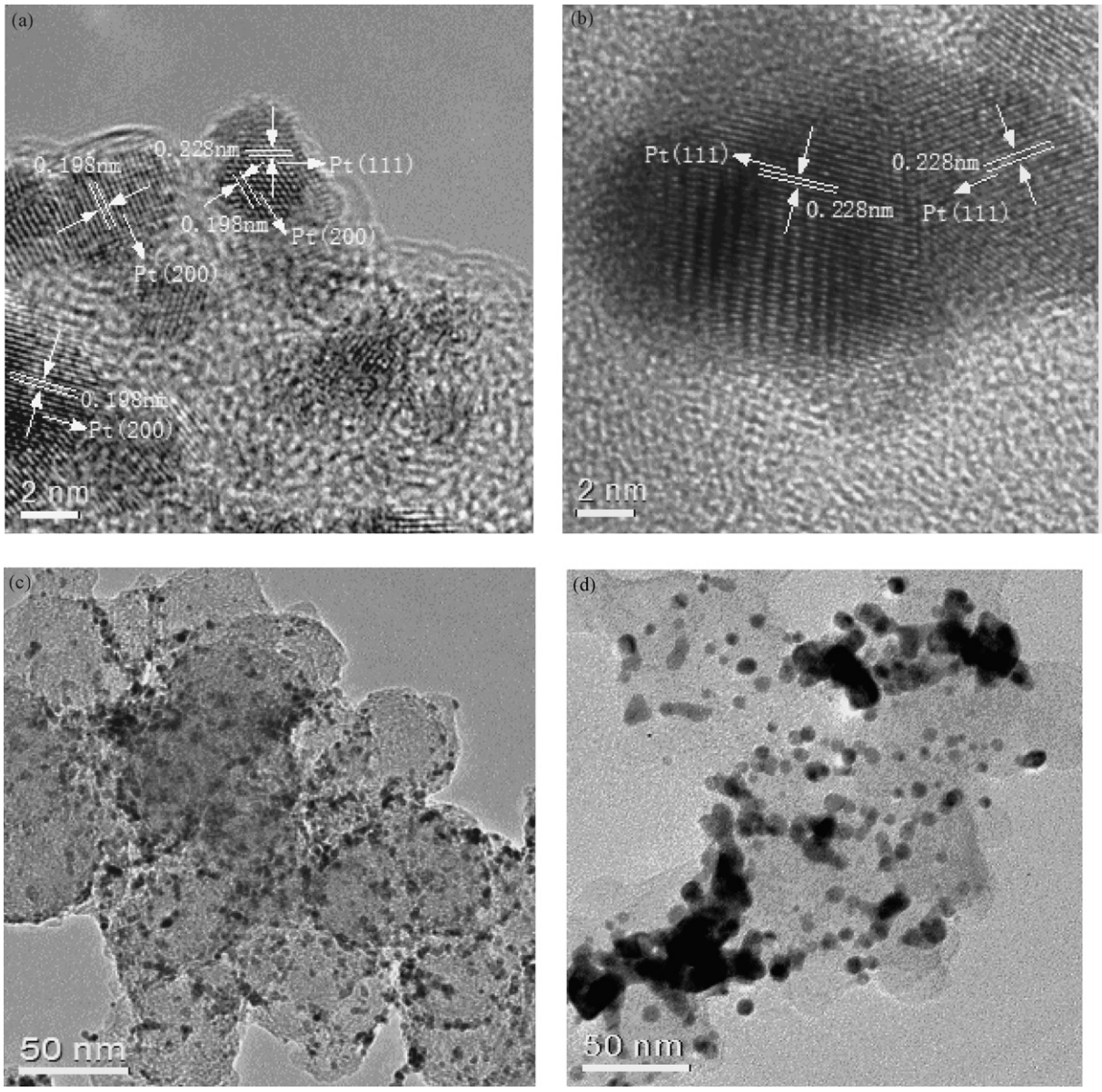

Fig. 10. HRTEM (a and b) and TEM (c and d) images of 40%Pt/XC-72 (JM) before (a and c) and after (b and d) 2020-h life-test.

polarization, IR drops and single cell performance are displayed in Fig. 7. After life test, the cell performance has dropped about 75% from 160 to 40 mW cm^{-2}. The cathode polarization seems to move to high potential during the first 556 h operation. Later, the oxygen reduction potential decreases linearly with the increasing test time under the same current density. These results show that the activity of cathode could be improved in first 556 h by discharging. But, under the cathode working potential in the range of 0.8–1.0 V versus DHE, Pt nanoparticles are unstable for agglomeration with cathodic degradation rate of 0.0335 mV h^{-1}. When fuel cell has worked over 2020 h, there appears an abnormal increase of cathode potential, which is due to that the cathode potential is not corrected by the mass transportation polarization. The IR drop increases linearly with discharging current improved, and the slope is equal to the value of internal resistance. With the test time increasing, the internal resistance becomes large, and the IR drop is more and more obvious for the lost of the cell voltage at the current density of 100 mA cm^{-2}.

The XRD patterns of the anode and cathode catalysts before and after test are shown in Fig. 8. All the catalysts show the characteristic diffraction peaks of Pt with face-centered cubic (fcc) structure. The peak around 26° can be attributed to (0 0 2) crystalline plane of carbon with hexagonal structure. Before the life-test, each of the diffraction peaks of Pt fcc structure of the anode catalyst shifts slightly to a higher 2θ value as compared with the cathode catalyst, and this is the result of the shrinking of the lattice parameter of Pt due to the alloying of Ru with Pt. In addition, the diffraction peaks of Pt become distinctly sharpen after the 2020-h life-test both for anode and cathode catalysts due to the agglomeration of metal particles on both electrodes. The crystalline lattice parameters and the particle

sizes as calculated by the Scherrer formula are listed in Table 2. It can be seen that the mean particle size of 40%Pt/XC-72 (JM) has grown from 3.31 to 6.28 nm, while that of 45%PtRu/XC-72 from 1.82 to 2.78 nm. The agglomeration of 40%Pt/XC-72 (JM) is more serious than that of 45%PtRu/XC-72. This is probably due to the higher working potential of the cathode than that of the anode (as shown in Fig. 7). Moreover, the lattice parameter of 45%PtRu/XC-72 prepared by the modified glycol method distinctly shrinks from 0.3876 to 0.3858 nm after life-test. The lattice parameter of 40%Pt/XC-72 (JM) has dilated slightly from 0.3914 to 0.3918 nm, and this is probably because the interaction between carbon support and Pt particle has become weaker after long time of discharging.

In order to study the change of microstructure of the anode and cathode catalysts after life-test, HRTEM and TEM images of 45%PtRu/XC-72 and 40%Pt/XC-72 (JM) are obtained and shown in Figs. 9 and 10, respectively. The histograms of the particles size distribution of the catalysts are shown in Fig. 11. It can be seen that the metal particles of both anode and cathode catalysts agglomerate distinctly to leave some part of carbon bare without metal particles coverage. Before the life-test, most of the metal particles of 45%PtRu/XC-72 and 40%Pt/XC-72 (JM) are around 2 and 3.5 nm, respectively. While after the 2020-h life-test, they increase to 3.5 and 5 nm, respectively. Some particles of 40%PtRu/XC-72 (JM) even have grown over 20 nm. These results show that the agglomeration of the cathode catalyst seems to be more serious than that of the anode catalyst, which is consistent to the results of XRD. The lattice planes of 45%PtRu/XC-72 and 40%Pt/XC-72 (JM) before and after the 2020-h life-test can be clearly distinguished from the HRTEM images. For the 40%Pt/XC-72 (JM) catalyst, the 0.228 and 0.198 nm spacings with a slight positive equipment error in Fig. 10a are assigned to the Pt (1 1 1) and Pt (2 0 0) planes (PCPDF#040802). After the life-test, the Pt (1 1 1) plane spacing increases very slightly to 0.229 nm (Fig. 10b). For the 45%PtRu/XC-72 catalyst before test, the 0.224 and 0.225 nm spacings assigned to Pt (1 1 1) plane (Fig. 9a) shrink distinctly as compared with the 0.228 nm spacing of the 40%Pt/XC-72 (JM) catalyst before life test (Fig. 10a), suggesting that some Ru has alloyed with Pt during the catalyst preparation process. After the life-test, the Pt (1 1 1) and (2 0 0) planes have the spacings of 0.223, 0.224 and 0.195 nm as shown in Fig. 9b, and the spacing of the relative planes seems not to change during life-test.

The composition and distribution of anode and cathode catalysts before and after life-test have been investigated by EDS and are shown in Fig. 12. The counts are proportional to the atomic concentration of elements and reflect changes of atomic

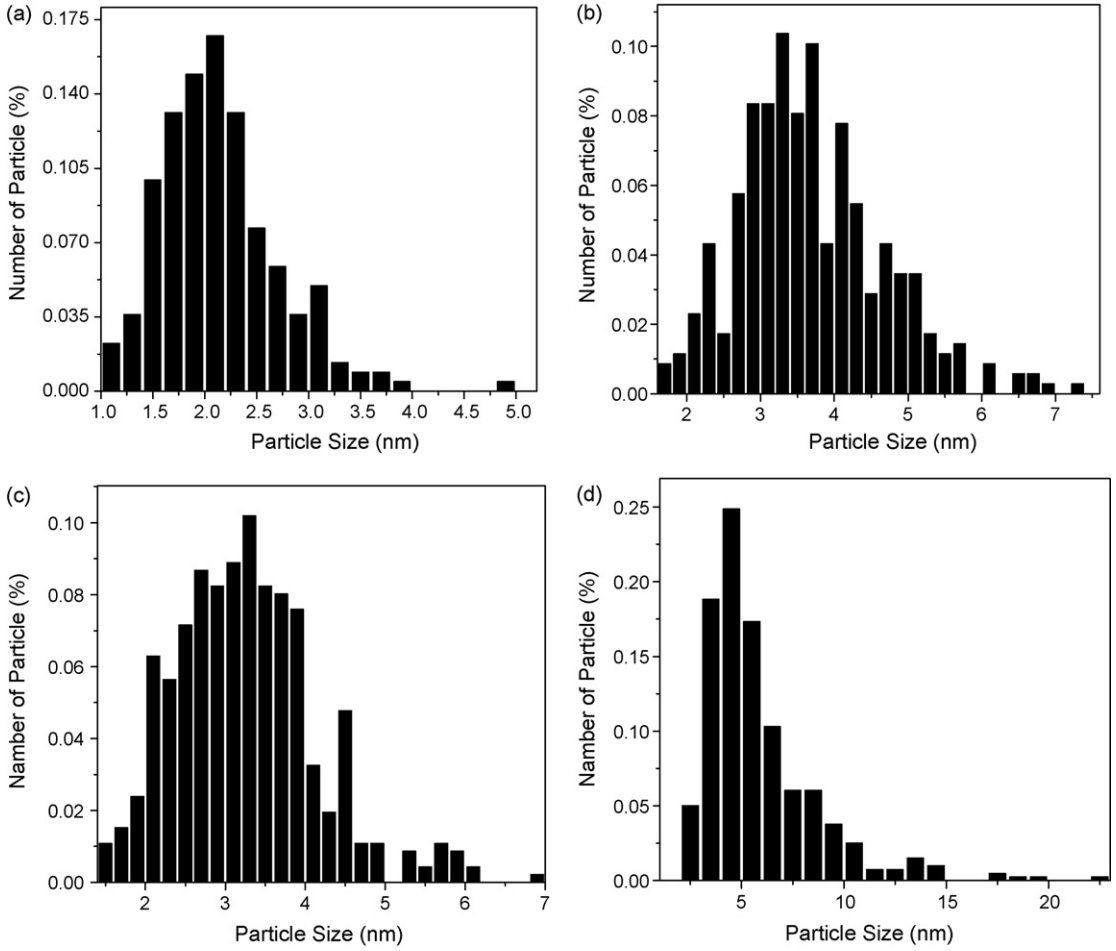

Fig. 11. Histograms of particles size distribution of 45%PtRu/XC-72 (a and b) and 40%Pt/XC-72 (JM) (c and d) before (a and c) and after (b and d) 2020-h life-test.

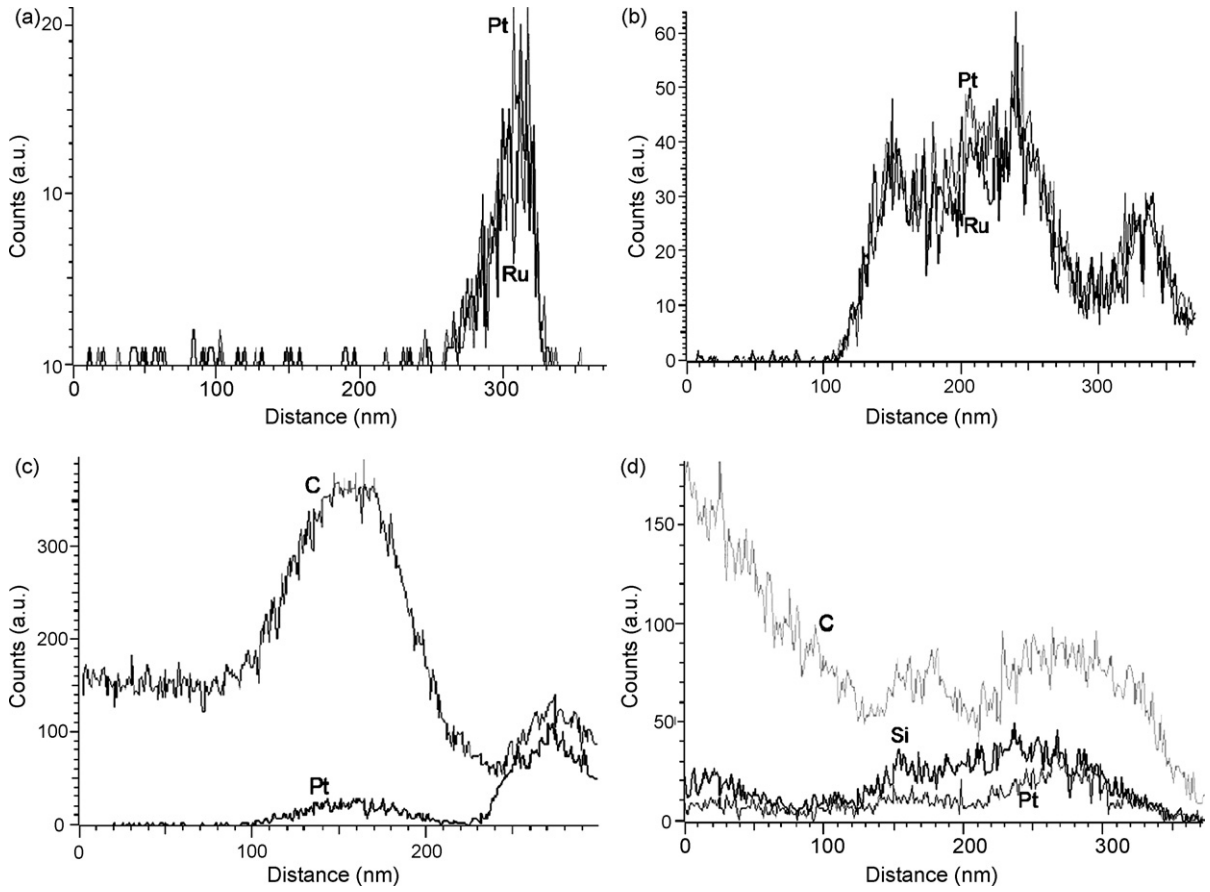

Fig. 12. The EDS results of 45%PtRu/XC-72 (a and b) and 40%Pt/XC-72 (JM) (c and d) before (a and c) and after (b and d) 2020-h life-test.

concentrations over the scanned distance. After the life-test, the composition profile of 40%Pt/XC-72 (JM) has changed. The presence of Si in the cathode catalyst has been reported [18], and is probably due to the leaching of silicon gasket under the oxidation atmosphere, but the influence of Si on the ORR activity of Pt/C is unclear. Moreover, Ru is not observed on the 40%Pt/XC-72 (JM) cathode catalyst as shown in Fig. 12d after the 2020-h life-test, which is inconsistent with the result reported by Chen et al. [5]. The reason is likely in that the cathode potential of this work is much higher than that reported by Chen et al. due to that the cathode of this work is fed with oxygen, while that reported by Chen et al. is fed with air. If Ru crossover could take place, Ru leaching at cathode is very easy under such high cathode potential (0.8–1.0 V versus DHE) in acid condition with long-term water rinsing. In contrast, for the 45%PtRu/XC-72 anode catalysts, the composition profile has also changed, and the EDS profiles show that Pt/Ru deviates from the nominal atomic ratio of 1:1, with Ru distinctly less than that of Pt from 170 to 230 nm as shown in Fig. 12b, which proves the leaching of Ru. Considering the alloying degree improvement as shown by XRD, the leached Ru is likely from the amorphous Ru. From the results of anode polarization and the curve of cell voltage versus life-test time, it is clear that the cell voltage gradually decreases and hardly recovers to the original level after the single cell discharges over 1093 h. Approaching to the end of the life-test, the voltage drop rate is increasing with test time, which is probably because the leaching rate of Ru is proportional to the anode potential when polarization potential is over 0.363 V versus DHE.

4. Conclusion

The durability of a DMFC with polyol-synthesized PtRu/C as the anode catalyst and a commercial Pt/C as cathode catalyst has been systematically and comprehensively studied by conducting a 2020-h life-test of a single cell discharging at a constant current density of 100 mA cm^{-2}. In anode, Ru leaching is the main reason for degradation. The results of anode polarization and EIS show that the stability of PtRu/C closely depends on the anode potential. Under an anode potential less than 0.363 V versus DHE, there exists a stable discharging period. When the anode potential exceeds 0.363 V versus DHE, the performance of the anode degrades dramatically due to the leaching of unalloyed Ru as shown by the EDS results. Thus, keeping a lower anode potential is essential to improve the life of a DMFC, which can be an important strategy for fabricating a DMFC to achieve a longer lifetime in the future. In cathode, it is observed that Pt nanoparticles are unstable with high aggregation and ripening under the cathode working potential in the range of 0.8–1.0 V versus DHE, leading to the drop of ESA and oxygen reduction polarization potential. From the results of EIS, the initial internal resistance increasing is probably due to the reduction of the

contact areas between the metal particles with carbon support and with Nafion ionomer, which are induced by the agglomeration of the metal particles of the electrocatalysts. However, when anode polarization potential exceeds 0.363 V versus DHE, the gradual leaching of the proton-conducting hydrous ruthenium oxides (RuO_xH_y) adds another mechanism for the increase of internal resistance.

Acknowledgements

We thank Prof. Ying Wan from Shanghai Normal University and Prof. Xuming Wei from Dalian Institute of Chemical Physics for the TEM analysis. This work was financially supported by Innovation Foundation of Chinese Academy of Science (K2006D5), Hi-Tech Research and Development Program of China (2006AA05Z137, 2006AA05Z139, 2006AA03Z225), National Natural Science Foundation of China (Grant No.: 50575036 and 50676093) and DUT-DICP Joint Research Foundation.

References

[1] K.B. Prater, J. Power Sources 61 (1996) 105–109.
[2] H. Dohle, H. Schmitz, T. Bewer, J. Mergel, D. Stolten, J. Power Sources 106 (2002) 313–322.
[3] S.C. Thomas, X. Ren, S. Gottesfeld, P. Zelenay, Electrochim. Acta 47 (2002) 3741–3748.
[4] X. Cheng, C. Peng, M. You, L. Liu, Y. Zhang, Q. Fan, Electrochim. Acta 51 (2006) 4620–4625.
[5] W. Chen, G. Sun, J. Guo, X. Zhao, S. Yan, J. Tian, S. Tang, Z. Zhou, Q. Xin, Electrochim. Acta 51 (2006) 2391–2399.
[6] J. Liu, Z. Zhou, X. Zhao, Q. Xin, G. Sun, B. Yi, Phys. Chem. Chem. Phys. 6 (2004) 134–137.
[7] A. Taniguchi, T. Akita, K. Yasuda, Y. Miyazaki, J. Power Sources 130 (2004) 42–49.
[8] W. Chen, G. Sun, Z. Liang, Q. Mao, H. Li, G. Wang, Q. Xin, H. Chang, C. Pak, D. Seung, J. Power Sources 160 (2006) 933–939.
[9] P. Piela, C. Eickes, E. Brosha, F. Garzon, P. Zelenay, J. Electrochem. Soc. 151 (2004) A2053–A2059.
[10] D.R. Rolison, P.L. Hagans, K.E. Swider, J.W. Long, Langmuir 15 (1999) 774–779.
[11] J.W. Long, R.M. Stroud, K.E. Swider-Lyons, D.R. Rolison, J. Phys. Chem. B 104 (2000) 9772–9776.
[12] L. Dubau, C. Hahn, C. Coutanceau, J.M. Leger, C. Lamy, J. Electroanal. Chem. 554-555 (2003) 407–415.
[13] Z. Wei, S. Wang, B. Yi, J. Liu, L. Chen, W. Zhou, W. Li, Q. Xin, J. Power Sources 106 (2002) 364–369.
[14] C. Eickes, P. Piela, J. Davey, P. Zelenay, J. Electrochem. Soc. 153 (2006) A171–A178.
[15] J.T. Muller, P.M. Urban, W.F. Holderich, J. Power Sources 84 (1999) 157–160.
[16] C. Cao, F. Scheiba, C. Roth, F. Schweiger, C. Cremers, U. Stimming, H. Fuess, L. Chen, W. Zhu, X. Qiu, Angew. Chem. Int. Ed. 45 (2006) 5315–5319.
[17] J. Guo, G. Sun, S. Sun, S. Yan, W. Yang, J. Qi, Y. Yan, Q. Xin, J. Power Sources 168 (2007) 299–306.
[18] S.-Y. Ahn, S.-J. Shin, H.Y. Ha, S.-A. Hong, Y.-C. Lee, T.W. Lim, I.H. Oh, J. Power Sources 106 (2002) 295–303.